

CINTAL - Centro de Investigação Tecnológica do Algarve
Universidade do Algarve

**Range-dependent acoustic tomography:
modeling an upwelling filament using
an asymmetric Gaussian function**

C. Soares and S. M. Jesus

Rep 05/03 - SiPLAB
18/Nov/2003

University of Algarve
Campus da Penha
8000, Faro,
Portugal

tel: +351-289800131
fax: +351-289864258
cintal@ualg.pt
www.ualg.pt/cintal

Work requested by	CINTAL Universidade do Algarve, Campus da Penha, 8000 Faro, Portugal tel: +351-289800131, cintal@ualg.pt,www.ualg.pt/cintal
Laboratory performing the work	SiPLAB - Signal Processing Laboratory Universidade do Algarve, FCT, Campus de Gambelas, 8000 Faro, Portugal tel: +351-289800949, info@siplab.uceh.ualg.pt, www.ualg.pt/fct/adeec/siplab
Projects	ATOMS - FCT, PDCTM/P/MAR/15296/1999
Title	Range-dependent acoustic tomography: modeling an upwelling filament using an asymmetric Gaussian function
Authors	C. Soares and S. M. Jesus
Date	November 12, 2003
Reference	05/03 - SiPLAB
Number of pages	21 (twenty one)
Abstract	This report describes a study to model an example of an upwelling filament of the California current system using a Gaussian function.
Clearance level	UNCLASSIFIED
Distribution list	SiPLAB(1), CINTAL (1), FCT(1)
Total number of copies	3 (three)

Copyright Cintal@2003

Contents

List of Figures	IV
1 Introduction	7
2 The CCS filament	9
3 Parameterization of the watercolumn	10
4 A synthetic study	12
5 GA search	14
6 Conclusion	20

List of Figures

2.1	<i>Range-dependent temperature profile in a region featuring an upwelling filament in the California current system [1].</i>	9
3.1	<i>Range-dependent temperature profile obtained in the interpolation step based on the temperature profiles measured at the edges of the waveguide.</i>	11
4.1	<i>Cost functions computed with the cross-frequency processor for the band 200 to 550 Hz. The cost functions were computed for (a) filament position and amplitude; (b) filament on set and off set rates.</i>	13
5.1	<i>Histograms obtained for the inversion using the canonic search bounds. The statistic is based on the 2 last generations of 50 independent populations.</i>	15
5.2	<i>Best filament estimation obtained in the first trial using the band 400 to 700 Hz.</i>	16
5.3	<i>Histograms obtained for the inversion using the altered search bounds (case 2 of table 5.2). The statistic is based on the 2 last generations of 50 independent populations.</i>	17
5.4	<i>Best filament estimation obtained in the second trial using the frequency band 400 to 700 Hz (case 2 of table 5.2).</i>	18
5.5	<i>Histograms obtained for the inversion using the altered search bounds higher frequencies (case 3 of table 5.2). The statistic is based on the 2 last generations of 50 independent populations.</i>	18
5.6	<i>Best filament estimation obtained in the third trial using the frequency band 750 to 1100 Hz (case 3 of table 5.2).</i>	19

Abstract

Acoustic tomography in range-dependent waveguides using a source-array pair represents an inverse problem with many potential solutions. The present problem is to model an upwelling filament which is a localized uprise of cold water and introducing a high degree of range dependence. In this study a parameterization scheme with a reduced number of parameters is proposed in order to represent the spatial evolution of the filament using an asymmetric Gaussian function parameterized by two variances, an amplitude coefficient and a mean value. Using a real data example of the filament of the Californian current system, this modeling scheme is tested on semi-synthetic data. The results indicate that such an approach can be considered for an efficient modeling of a complex oceanographic feature.

intentionally blank

Chapter 1

Introduction

The ATOMS project aims at applying the Ocean Acoustic Tomography (OAT) concept to the monitoring of upwelling filaments. A filament constitutes a spatial anomaly in the water column temperature profile that corresponds to a deep cold water mass raising to the surface. Thus, a waveguide containing a filament constitutes a range-dependent environment for acoustic propagation.

An estimation problem with a range-dependent underlying environment using a vertical array has potentially many solutions. Eventually, one has to proceed such that enough constraints are introduced into the problem and therefore enable the environmental model to achieve a sufficient degree of uniqueness. This requires a great deal of *a priori* information to be included in the estimation problem in order to highly reduce the number of solutions. A common difficulty in underwater acoustic estimation problems is the high number of unknown parameters that must be estimated. There are a number of configurations of the unknown parameters that induce an high number of degrees-of-freedom, which means that different estimates of the unknown parameter set can have similar acoustic responses. Upwelling filaments are ocean features that are usually present in coastal regions [1, 2]. In Ref. [3] a study regarding the detection of an upwelling filament and tracking its variability was carried out using standard sound-speed profiles. The environment was parameterized with boundaries at the on set and off set of the filament, and a coarse representation with few points was used. Under this simple configuration it was found that the cost function was sensitive enough to all the parameters used to represent the filament.

An emerging tool to solve multiple parameter estimation problems in ocean acoustics is *Matched-Field Tomography* (MFT) [4]. This technique was adopted from *Matched-Field Processing* (MFP) [5]. MFP was first used for range-depth source localization, but the emergence of the *focalization* concept [6] and the rapid growth of computational facilities allowed extending this technique to virtually any parameter of interest. MFT stands therefore for a matched-field problem where the properties of interest are in the watercolumn such as temperature and salinity. The more classic approach of travel-time tomography is best suited for large scale problems and deep water areas [7].

This report describes a filament parameterization scheme that has been based on a visual observation of a filament measured in the California current system (CCS) [8]. This scheme explores the features and shape of that filament in order to define a physical model and respective parameterization. Then the viability of the proposed parameterization is inspected using semi-synthetic acoustic data. Parameter estimation results using real range-dependent temperature profiles are reported. The results suggest that it is possible

to design a physical model for the California current system example and obtain accurate position, amplitude coefficient, and values of on set and offset of the upwelling filament.

Chapter 2

The CCS filament

Eastern ocean boundaries are regions of high upwelling occurrence. The plot in figure 2.1 shows a filament measured in the Californian current system. This was the only temperature measurement containing a filament available until now. Most knowledge about the formation of the upwelling filaments, their spatial structure and their mass transportation was obtained from measurements performed during the Coastal Transition Zone Program in the CCS. Some authors reported strong similarities between the basic circulation patterns of the CSS and the Iberian peninsula [1, 2]. According to the studies specific to this region, the upwelling season starts in May or June, where fingers of cold water grow into filaments that typically reach the maximum length and width of 250 km and 50 km respectively.

The CCS filament has an upwelling visible between ranges of 50 and 130 km. The filament shows some features that can be explored in order to design an appropriate physical model and respective parameterization. The present problem consists in estimating temperature profiles that are between the acoustic source and the vertical array. The phenomena has to be modeled with a number of parameters that enables the inverse problem to be carried out with enough constraints in order to preserve the uniqueness of the solution, while minimizing the environmental mismatch.

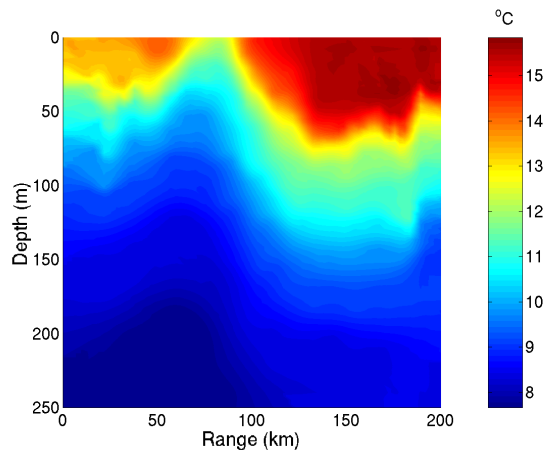


Figure 2.1: *Range-dependent temperature profile in a region featuring an upwelling filament in the California current system [1].*

Chapter 3

Parameterization of the watercolumn

A filament represents an environmental anomaly in the propagation channel where it is contained. Roughly, it is a localized displacement of a cold water mass that might even be visible at a surface e.g. by a satellite. Thus, if a portion of environment containing the filament is considered, three important regions can immediately be identified: a sector between the source and the filament (sector 1), the filament itself (sector 2), and a sector between the filament and the vertical array (sector 3). Consequently, the present case represents a range-dependent environment.

The most obvious properties of the present case are the ranges of the beginning and the end of the filament. Another pertinent question can be raised: how to model the filament itself? It does not represent abrupt changes in the water temperature, but rather changes that are progressive with range. Visual observation suggests a progressive raise of the thermocline either from the source end, either from the array end, until it reaches the minimum depth (yellow color). A closer observation indicates that not only the thermocline raises, but an uniform displacement of each temperature profile takes place. This displacement is almost linear with range, but at the edges and the center it shows a curvature, that makes the amount of displacement as a function of range to be comparable with a Gaussian function. The concept of the monitoring system assumes that temperature profiles measured at the acoustic source and the vertical array locations are available. Another important characteristic of the present data is that the portions away of the filament can be considered nearly range-independent or mildly range-dependent. Furthermore, the temperature profiles to the source end and to the array end of the filament are different. This might be very important in order to impose constraints in the position of the filament, since the acoustic field might be able to discriminate the lengths of sector 1 and sector 3. However, care must be taken, since at 190 km a strong raise in the thermocline is visible.

After the observations above, it follows that two Gaussian functions will be used to represent the displacement observed in the temperature profiles - one defined in the zone from the source position to the filament position, and the other in the zone from the filament position to the array location. The reason for this is to allow different rates of profile displacement. Thus the filament (Gaussian function) will be parameterized with four unknowns:

- Filament position m ;
- Filament amplitude A ;

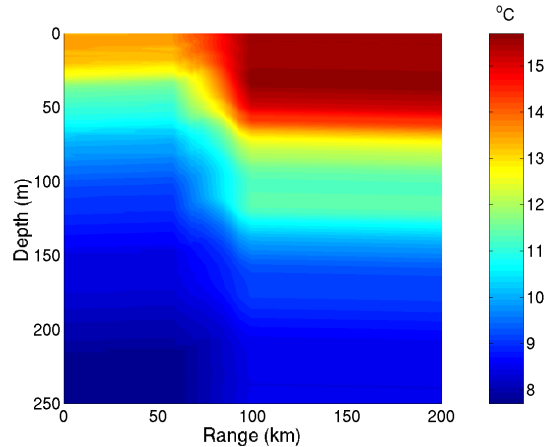


Figure 3.1: *Range-dependent temperature profile obtained in the interpolation step based on the temperature profiles measured at the edges of the waveguide.*

- On set and off set rates σ_s and σ_a .

The subscripts s and a stand respectively for “source end” and “array end”. By using a Gaussian function one can assume that the filament starts at range zero and extends to the array location, since a Gaussian function falls off rapidly to zero as the independent variable leaves the center of the function. Both half-functions have A as maximum amplitude and are centered at range m in order to avoid a discontinuity at that point:

$$f(r) = \begin{cases} Ae^{-\frac{(r-m)^2}{\sigma_s^2}} & r \leq m \\ Ae^{-\frac{(r-m)^2}{\sigma_a^2}} & r > m \end{cases} \quad (3.1)$$

where $f(r)$ is continuous in r . The parameters of this function are to be optimized using a genetic algorithm (GA). Then, of course the source range and depth must be included as free parameters in order to allow enough degrees-of-freedom to mitigate modeling mismatch.

In general, the model will be able also to adjust the size of the range sectors. There will be two long sectors 1 and 3, and then many short range-independent sections in cold water uprushing region, whose size will be adapted to the derivative of the underlying Gaussian function. This procedure is fundamental to limit the computation cost of each model to the strictly necessary by limiting the number of subsections.

Finally, an important issue is the junction of the two long range-independent sectors. Since the filament represents an anomaly in the water column temperature profile with a smooth evolution over range, it will also reflect the temperature profiles to the source end and to the array end, and can be viewed as a transition region from sector 1 to sector 3. The estimation of the filament is based on the temperature profiles measured at the source location and array locations, which are used respectively in sectors 1 and 3. Thus, for each hypothetical parameter set, the derivative of the respective underlying Gaussian function is first calculated, in order to efficiently divide the whole propagation channel into sectors. Then the *transition profiles* are obtained by linearly interpolating temperature values with same depths between ranges at the end of sector 1 and the beginning of sector 3. An example of the result of this preliminary step is shown in figure 3.1.

Chapter 4

A synthetic study

In MFP it is fundamental to ensure that solutions are unique. This happens if no environmental mismatch and noise are present or the spatial Nyquist sampling rate is satisfied. Although non of these conditions are fully satisfied in practical cases, the realistic conditions often still allow MFP to be performed with a satisfactory degree of success, i.e. for example in a range-depth plane it is possible to obtain the maximum matched-field response for the true source position. Note that the range-depth plane has more commonly been called ambiguity surface, in order to reflect the fact that a number of solutions can yield acoustic responses that closely match the response of the true solutions.

However, in a more generic estimation problem, i.e., a scenario with multiple unknowns, of diverse types, e.g., geometric parameters to be estimated together with temperature profiles, the ambiguity pattern is certainly different, and perhaps even more ambiguous than that encountered in a range-depth ambiguity function. Thus, it is instructive to calculate functions that depend on the parameters to be estimated, in order to get an insight about the sensitivity of the cost function on the parameters. Of course, the best that can be done is to plot functions of two parameters.

The data was generated using the CCS filament conditions and respective waveguide with a waterdepth of 250 m and typical values for the bottom. The position and the amplitude of the filament were respectively set to 80 km and 50 m by visual inspection of figure 2.1, and source range and depth 200 km and 125 m respectively. The filament extensions σ_s and σ_a were respectively set to 14.66 and 10.49 km, by previously carrying out an optimization with the CCS filament fixing the remaining parameters to the values given above.

The vertical array has 16 receivers spaced by 4 m and distributed between 95 and 155 m, and the field was simulated at frequencies 200 to 550 Hz with a 50 Hz resolution with no noise using the C-SNAP normal-modes propagation model [9]. The cost function used to study the sensitivity was the cross-frequency Bartlett processor [10].

Figure 4.1(a) shows the ambiguity surface obtained for the filament position and amplitude. It can be seen that the peak at the correct position is very narrow which suggests the high sensitivity of the acoustic field relative to these parameters, although many narrow sidelobes are observed in the background. This can be interpreted by the fact that the temperature profiles are well known in sectors 1 and 3, which is *a priori* information representing a strong constraint in terms of possible solutions for the inverse problem.

Concerning the filament extensions, it can be seen in figure 4.1(b) that the field is very

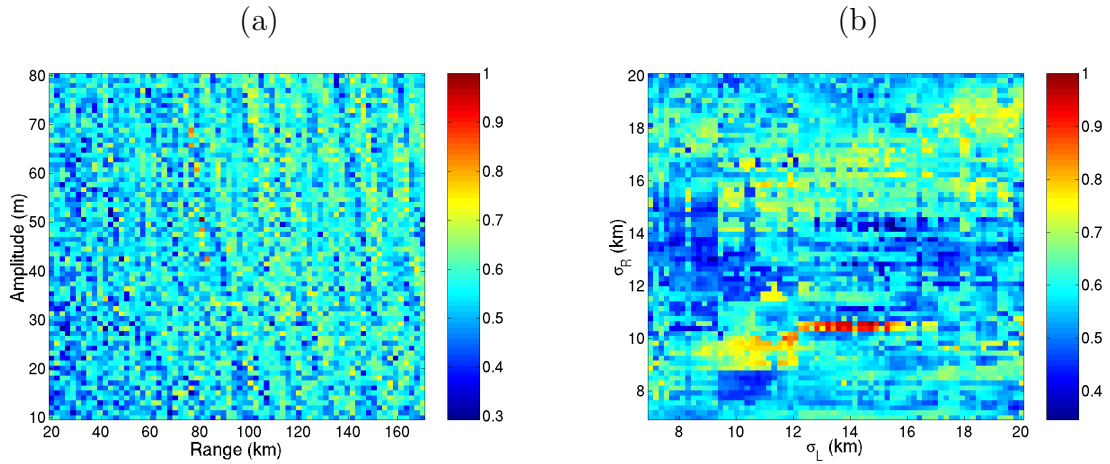


Figure 4.1: *Cost functions computed with the cross-frequency processor for the band 200 to 550 Hz. The cost functions were computed for (a) filament position and amplitude; (b) filament on set and off set rates.*

sensitive to the off set rate, but suffered a very smooth evolution with the on set rate. This can perhaps be explained by the position of the filament and the depth of the thermocline on the source end and array end of the filament.

Chapter 5

GA search

Semi-synthetic data has been generated in order to test the modeling in the context of a global search using a GA [11]. The environmental conditions are the same as those encountered in section 4 except for the frequencies processed. Two tests will be performed: in the first test the frequencies were in the band 400 to 700 Hz, and in the second test in the band 750 to 1100 Hz in both cases with a frequency resolution of 50 Hz.

This optimization included two geometric parameters (source range and depth) and the four parameters modeling the filament. Table 5.1 shows their search bounds and quantization steps. Although the data is synthetic and it is assumed that the source location is accurately known, relatively large search intervals were chosen for source range and depth, in order to allow these parameters to vary and eventually compensate inherent environmental mismatch. The number of generations was set to 40 and the population size to 80. Crossover and mutation probabilities were set to 0.8 and 0.007, respectively.

The test of the GA with this configuration of unknown parameters aims at testing the viability of this modeling scheme in terms of environmental model adjustment. The semi-synthetic acoustic data is suitable for a mismatch study, since the only source of mismatch is eventually the filament itself. This parameter configuration can potentially yield a very ambiguous multi-dimensional ambiguity function, which is to be maximized using a GA. In the presence of environmental mismatch even the controlled parameters such as source location become unknown. Thus, it is not possible to know *a priori* what are the true parameters to be obtained, since such mismatch is to be compensated by allowing those parameters to assume values that are not the true values. In order, to get an idea about the ambiguity pattern of such multi-dimensional ambiguity function, one

Model parameter	Lower bound	Upper bound	Quantization step
Geometric			
source range (km)	190	210	256
source depth (m)	100	150	64
Filament			
filament range (km)	30	120	128
amplitude (m)	20	80	128
on set rate σ_s (km)	7.07	18.71	256
off set rate σ_a (km)	7.07	18.71	256

Table 5.1: *GA forward model parameters with search bounds and quantization steps.*

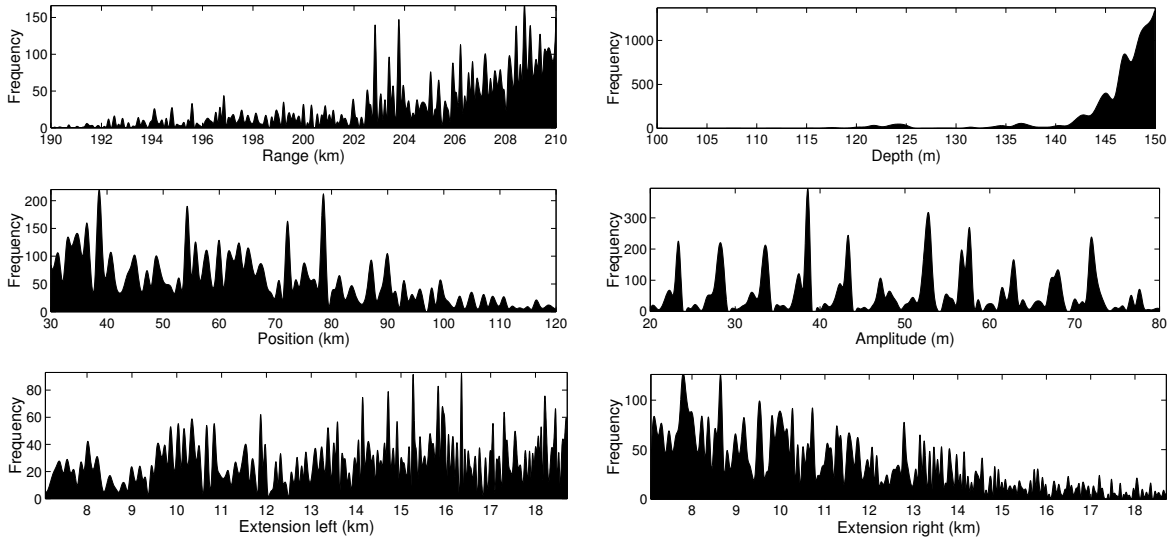


Figure 5.1: *Histograms obtained for the inversion using the canonic search bounds. The statistic is based on the 2 last generations of 50 independent populations.*

can proceed with a statistical approach. In the context of *a posteriori probabilities* [12, 13], the computation of histograms of the parameters obtained from the last generations of the GA search can give an indication of how well determined the parameters are.

In the present study only a single measurement of the upwelling filament is available. In order to obtain results with statistical relevance inversions with 50 independent populations were carried out. Figure 5.1 shows histograms for the six parameters under estimation obtained using all individuals of the two last generations of each independent population. The first row corresponds to the source location. It can be clearly seen that the solutions with highest fit are those with source range above 200 km and source depth above 140 m. The geometric mismatch is obviously induced by the filament modeling mismatch. The distribution of the filament position is spread over the search interval with the highest peaks at 38.5 and 78.5 km. The amplitude distribution is also spread over the whole search interval but there are well defined peaks every 5.5 m and a peak with good outstanding at 38.5 m. The filament extension distributions are also spread, but the distribution for the off set rate for most of the individuals considered is below 200.

The best fit found in the 50 inversions is 0.83, which is relatively high. Although the distribution for source range suggests that the parameters could be well above 200 km, its estimated value was 196.27 km. Table 5.2 shows the best individual for the three inversion attempts. The obtained profile is shown in figure 5.2.

In the second attempt the search interval for source depth was set between 120 and 170 m in order to allow estimates above 150 m depth to be tested. All other search intervals were the same as in the first attempt. It can be seen that the distribution for the source depth is well concentrated in the interval between 145 and 157 m, and the source range is more concentrated in the vicinity of 210 km range (see figure 5.3). All the other parameters show approximately the same distributions.

The best fit found in the 50 inversions is again 0.83 corresponding to the parameter vector designated as Case 2 in table 5.2. This result indicates that there is an high degree of ambiguity, and that the physical modeling suggested might be unable to represent the reality with an high degree of accuracy and sufficient degree of uniqueness. The obtained

Model parameter	Case 1	Case 2	Case 3
Geometric			
source range (km)	196.27	209.4	209.1
source depth (m)	142.9	151.0	138.3
Filament			
filament range (km)	74.6	73.2	110.8
amplitude (m)	43.1	52.1	52.1
on set rate σ_s (km)	13.7	13.6	14.5
off set rate σ_a (km)	11.5	14.2	10.3

Table 5.2: *Best individuals obtained during the GA search for the three inversion attempts.*

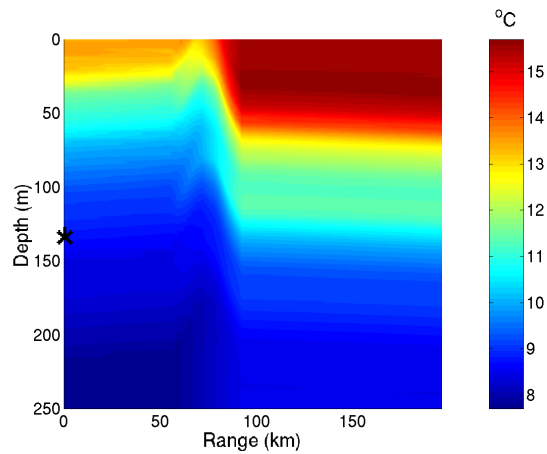


Figure 5.2: *Best filament estimation obtained in the first trial using the band 400 to 700 Hz.*

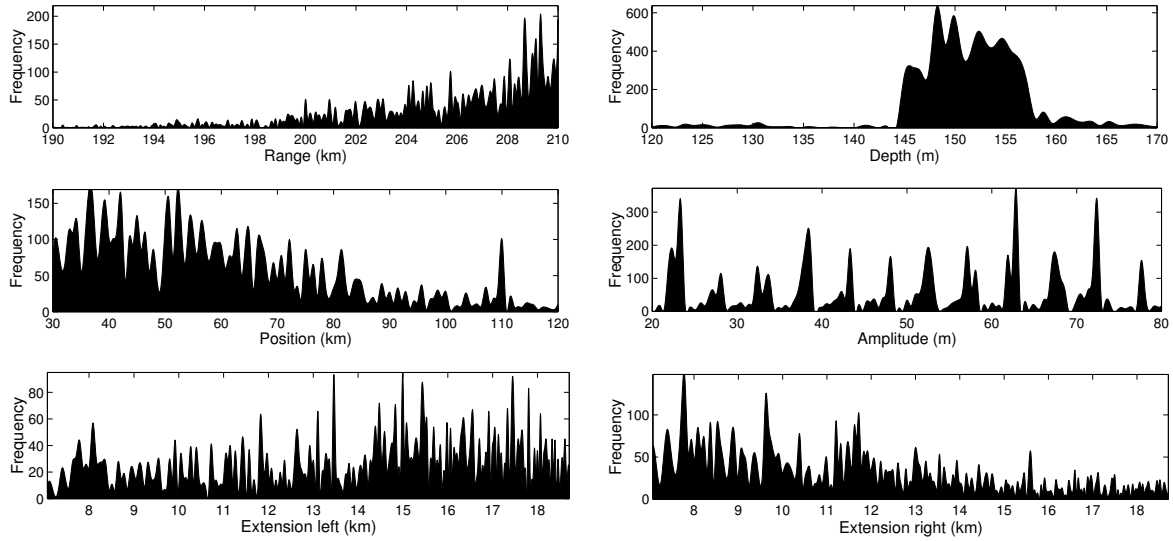


Figure 5.3: *Histograms obtained for the inversion using the altered search bounds (case 2 of table 5.2). The statistic is based on the 2 last generations of 50 independent populations.*

profile is shown in figure 5.4.

In another test the higher frequency band was used in order to increase the degree of uniqueness. It can be seen that using a higher frequency band did not contribute significantly in terms of convergence to a solution, where the final generations are even more widely spread over the search space (figure 5.5). However, concerning the best individual found, it can be seen in table 5.2 that source range and filament amplitude are coincident, while source depth and left extension are consistent. The filament position was estimated too far from its true position. The best fit was 0.69, and decreased due to increase in frequency, which increases the sensitivity of the matched-field response with the mismatch. The obtained profile is shown in figure 5.6.

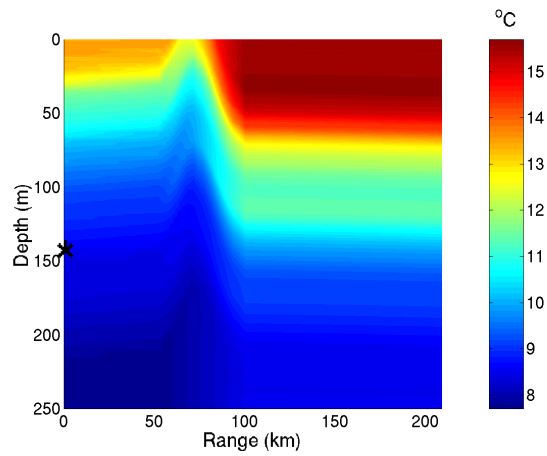


Figure 5.4: *Best filament estimation obtained in the second trial using the frequency band 400 to 700 Hz (case 2 of table 5.2).*

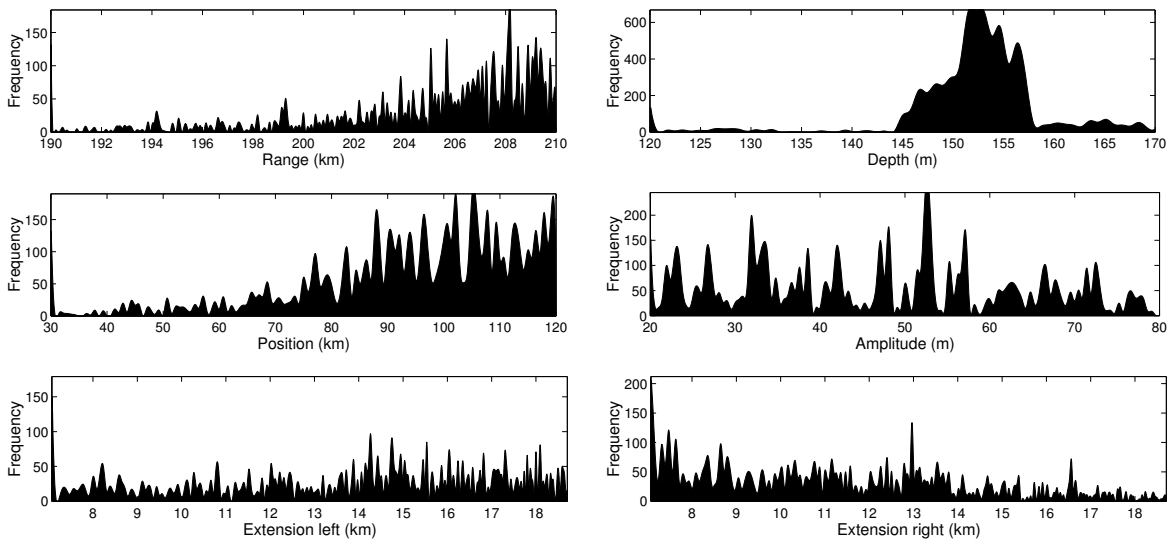


Figure 5.5: *Histograms obtained for the inversion using the altered search bounds higher frequencies (case 3 of table 5.2). The statistic is based on the 2 last generations of 50 independent populations.*

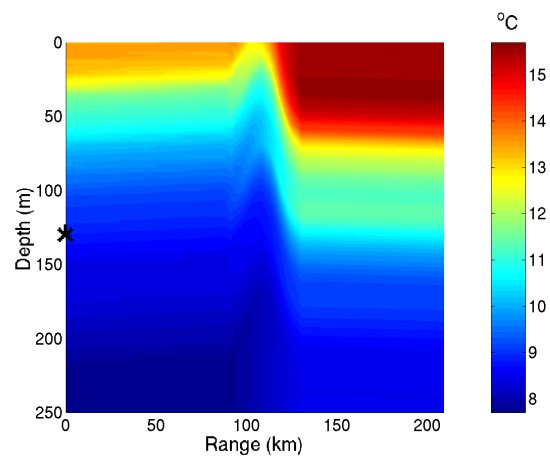


Figure 5.6: *Best filament estimation obtained in the third trial using the frequency band 750 to 1100 Hz (case 3 of table 5.2).*

Chapter 6

Conclusion

An upwelling filament is a cold mass of water that raises from deep layers of the water column towards the surface. In the context of an acoustic propagation channel it represents an anomaly of the sound-speed over range. Thus, a waveguide containing a filament is a range-dependent environment. It is difficult, in the framework of acoustic tomography, to deal with range-dependency in a typical experimental setup of a single sound source-array pair, since the inverse problem for parameter estimation has potentially many solutions.

The present problem consists in estimating temperature profiles laying between the acoustic source and the vertical array. Therefore, an efficient parameterization was developed in order to keep a low number of parameters preserving the ability to represent the range-dependency of the water column temperature. Two Gaussian functions were used to represent the non-symmetric shaped range-dependent thermocline resulting in a parameterization of four parameters.

Two inversion attempts were performed for a lower frequency band, and a third inversion attempt was performed for a higher frequency band. The inversion results indicate that a significant ambiguity among solutions is present. The histograms taken from the individuals of the GA show a high dispersion of the parameter in general, and for the filament parameters in particular, although some outstanding peaks are visible. In the first two inversion trials the position and amplitude was within the expected values for the best fit parameter vector. No environmental validation is presented in this study, but it is possible to use the source location estimates to get a feeling of the degree of mismatch: in the first attempt the source range is estimated 2% below the correct range, and 5% in the other attempts; the source depth is best estimated for the higher frequencies since both error for the highest fit and dispersion are smaller in this case.

The results show that it is possible to locate and estimate the shape of a filament with its maximum amplitude under realistic conditions using an acoustic source and a vertical array. In the future other parameterization schemes should be tested in order to reduce the mismatch inherent to the rigidity of the present choice.

Bibliography

- [1] R. Haynes. *Eulerian and lagrangian observations in the Iberian coastal transition zone*. PhD thesis, Univ. of Wales, Bangor, 1993.
- [2] P. Relvas. *The physical oceanography of the Cape São Vicente upwelling region observed from sea, land and space*. PhD thesis, Univ. of Wales, Bangor, 1999.
- [3] V. Corr and S. Jesus. Tracking cold water upwelling filaments in the oceans using matched-field inversion. *Acta Acustica*, 89:604–613, 2003.
- [4] A. Tolstoy, O. Diachok, and L. N. Frazer. Acoustic tomography via matched field processing. *J. Acoust. Soc. Am.*, 89(3):1119–1127, 1991.
- [5] M. J. Hinich. Maximum-likelihood signal processing for a vertical array. *J. Acoust. Soc. Am.*, 54:499–503, 1973.
- [6] M. D. Collins and W. A. Kuperman. Focalization: Environmental focusing and source localization. *J. Acoust. Soc. America*, 90:1410–1422, 1991.
- [7] W. Munk, P. Worcester, and C. Wunsch. *Ocean Acoustic Tomography*. University Press, Cambridge, 1995.
- [8] P. T. Strub, P. M. Kosro, and A. Huyer. The nature of the cold filaments in the California Current System. *J. Geophysical. Res.*, 96(C8):14743–14768, 1991.
- [9] C. M. Ferla, M. B. Porter, and F. B. Jensen. C-SNAP: Coupled SACLANTCEN normal mode propagation loss model. Memorandum SM-274, SACLANTCEN Undersea Research Center, La Spezia, Italy, 1993.
- [10] C. Soares and S. M. Jesus. Broadband matched field processing: Coherent and incoherent approaches. *J. Acoust. Soc. Am.*, 113(5):2587–2598, May 2003.
- [11] T. Fassbender. *Erweiterte genetische algorithmen zur globalen optimierung multimodaler funktionen*. Diplomarbeit, Ruhr-Universität, Bochum, 1995.
- [12] D. F. Gingras and P. Gerstoft. Inversion for geometric parameters in shallow water: Experimental results. *J. Acoust. Soc. America*, 97:3589–3598, 1995.
- [13] P. Gerstoft and D. F. Gingras. Parameter estimation using multi-frequency range-dependent acoustic data in shallow water. *J. Acoust. Soc. America*, 99:2839–2850, 1996.